ARTICLES

Molecular Modeling of Interactions in Zeolites: An Ab Initio Embedded Cluster Study of NH$_3$ Adsorption in Chabazite

James M. Vollmer, Eugene V. Stefanovich, and Thanh N. Truong*

Henry Eyring Center for Theoretical Chemistry, Department of Chemistry, University of Utah, 315 S. 1400 E., Room Dock, Salt Lake City, Utah 84112

We present an embedded cluster approach for modeling interactions in zeolites and an application of this model to the study of NH$_3$ and NH$_4^+$ adsorption in chabazite. This model utilizes the SCREEP (surface charge representation of the electrostatic embedding potential) formalism to include an accurate description of the Madelung potential in quantum mechanical calculations. The model is validated by comparison with previous cluster, embedded cluster, and periodic calculations on this system. The importance of including the Madelung potential and geometry relaxation in zeolite calculations is addressed. After considering the effects of electron correlation, basis set superposition error, and the zero-point energy, the model yields a heat of adsorption of −170 kJ/mol for NH$_4^+$ in chabazite, in good agreement with experimental TPD data.

Introduction

Zeolites play an increasingly important role as catalytic materials in petroleum refining, synfuel production, and petrochemical production. It is well accepted that their catalytic activity is primarily due to the high acidity of zeolite Brønsted sites, which bridge hydroxyl groups neighboring aluminum substitution sites. Because of this importance, numerous studies have investigated the interactions of these acidic sites with a wide range of probe bases.[1−3] Experimentally, these interactions are generally probed with microcalorimetry, temperature-programmed desorption,[2,4] and IR and NMR spectroscopies;[5−12] theoretically, they are modeled mainly by small quantum clusters interacting with the probe molecules in what is referred to as the cluster approach.[1−3,13−15]

In the cluster approach, the zeolite is represented by a small neutral cluster containing the Brønsted acid site. Hydrogens are used to cap unsaturated bonds. Then the cluster is treated like isolated gas-phase molecules, and the properties available in standard ab initio packages can be calculated (energetics, geometry minimizations, frequencies, and NMR shifts). The results are reasonable for some cases, however, their accuracy is limited by the following factors: (1) if no constraints are placed on the boundary atoms of the cluster, the cluster is unrealistically flexible; (2) if the geometry is allowed to relax, the presence of the terminating hydrogens can lead to the formation of artificial hydrogen bonds on the cluster's boundary; (3) no contributions from the extended zeolite are included, eliminating the ability to model the effects of various Si/Al ratios or countercations, as well as the ability to model steric effects due to the zeolite structure.

One way to overcome the mentioned limitations in the cluster model would be to make use of periodic boundary conditions such as in periodic Hartree−Fock (HF) or density functional theory (DFT) and to model the entire infinite zeolite quantum mechanically. Interactions with the probe molecule would then correspond to the high loading case. This approach, however, faces different limitations. The most serious one is that the unit cells of zeolites are often too large to be computationally tractable. This fact makes only small basis sets feasible and limits the applicability of these methods to zeolites with very small unit cells, such as chabazite which has 36 atoms/unit cell; industrially important zeolites (e.g., zeolite Y, which has approximately 576 atoms/unit cell) would be extremely costly, if even feasible with current computer technology.

To overcome the computational limitations of periodic methods, while accounting for the crystal effects of the zeolite, two general embedding schemes have been developed: "electronic" and "mechanical." The most rigorous treatment of the electronic embedding scheme includes quantum mechanical effects, electrostatic Coulombic and exchange contributions between the cluster and the crystal environment. This is done by utilizing Green function techniques to "embed" the cluster wave function, of the defect site or site of interest, in the environment of the unperturbed crystal's wave function.[16] Most electronic embedding schemes, however, focus only on including the electrostatic interactions of the remaining zeolite in the Fock matrix of a quantum mechanical cluster, effectively "embedding" the cluster in the external classical electrostatic potential. Several methods have been developed for representing this electrostatic potential including: (1) embedding the cluster in a finite set of lattice point charges,[17] where formal charges, half-formal charges, or charges derived from population analyses of cluster calculations are used; adding the Madelung potential of the zeolite to the Fock matrix of the cluster as a series of multipole expressions;[18] and embedding the cluster in a finite set of point charges, which are derived to represent the
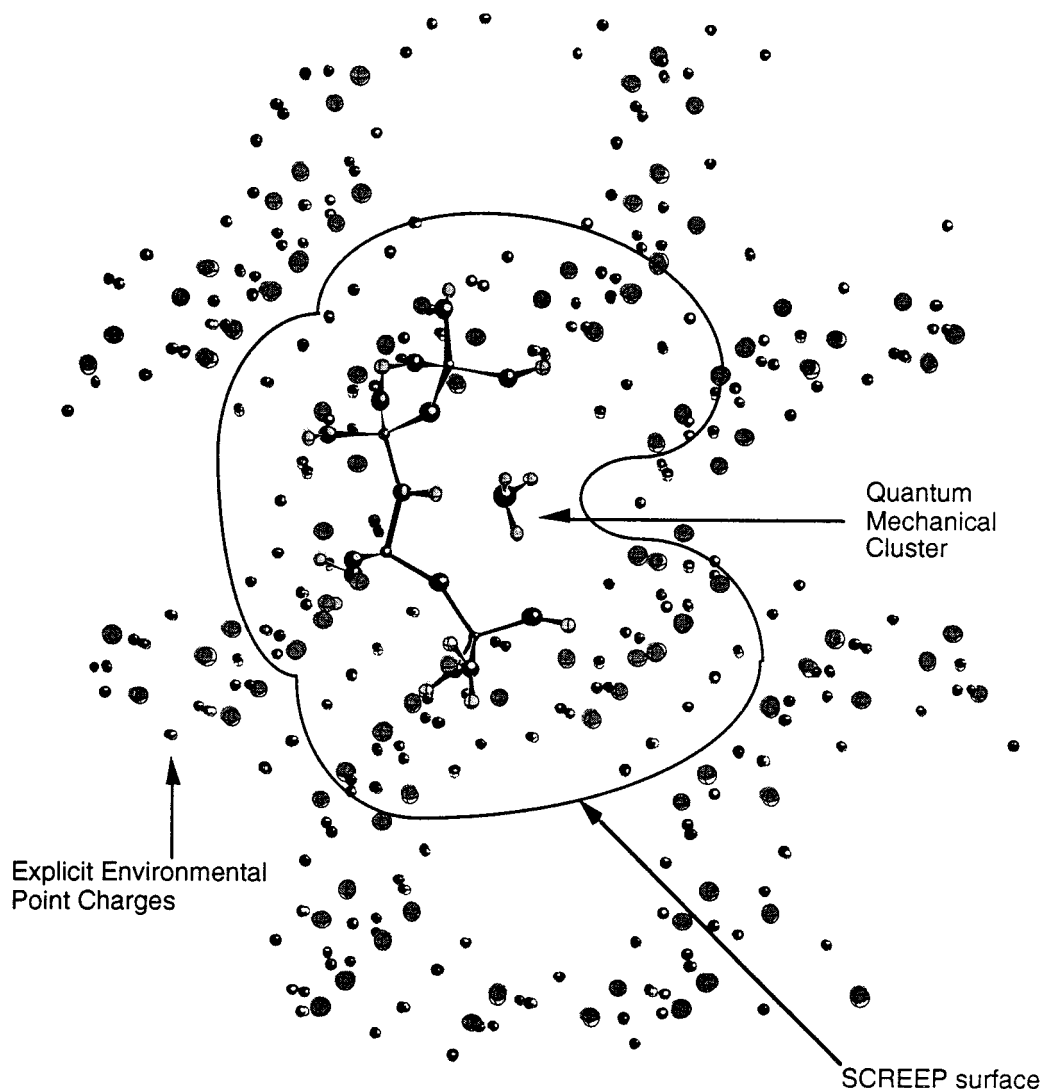
Figure 1. Embedded cluster model for studying adsorption in zeolites.

Madelung potential.[19] Alternatively, mechanical embedding procedures represent the crystal environment as an analytical force field and the defect site is treated as a quantum mechanical cluster. Here the electrostatic potential of the crystal environment is not included in the Fock matrix of the cluster, thus it does not polarize the cluster's wave function directly but rather affects the cluster's geometry and subsequently the cluster's wave function. Perhaps the most widely known of these mechanical embedding procedures is the IMOMM formalism introduced by Maseras and Morokuma.[20] Recently, Brändle and Sauer applied their mechanical embedding scheme to the study of NH_3 adsorption in faujasite and achieved a promising prediction for the heat of formation of NH_4^+ in faujasite,[21] which may cause some debate over the importance of including electrostatic contributions in the Fock matrix for embedded cluster calculations.

Recently our lab has proposed a methodology for accurately representing the Madelung potential in ab initio calculations. This embedded cluster methodology has been applied successfully to various metal oxide systems,[22,23] and here it is our goal to demonstrate its applicability to the study of zeolites. For this purpose we investigated the chabazite/NH_3 system, which is becoming the standard test case for embedded cluster model development in zeolites. In the "Methodology" section, we present the general formulation of our embedded cluster model

and describe the computational details common to all subsequent sections. In the "Results" section we address four important issues. First, we investigate the accuracy of our representation of the Madelung potential, by comparing the potential for our embedded cluster, the bare cluster, and periodic calculations. Second, we attempt to validate our model for the study of adsorbate/zeolite interactions by reproducing potential energy sections for head-on adsorption of NH_3 and NH_4^+ at a chabazite Brønsted site, for comparison with previously reported embedded, periodic, and bare cluster results.[16,18,24] Third, we address the importance of the choice of environmental embedding charges by repeating these potential energy section calculations using three different sets of environmental embedding charges. Last, we look at the importance of structural relaxation by optimizing our embedded cluster. In the "Discussion" section we compare our optimized results with previous embedded and experimental results[4,25] and assess our method's ability to model this and similar systems.

Methodology

Embedded Cluster Model. Our embedded cluster has three layers (see Figure 1). At the center of our model is a quantum mechanical cluster, "cut" from the zeolite framework, around the site of interest. Due to the partial covalent nature of zeolites,

hydrogens are used to terminate the cluster's dangling bonds, to saturate electronic spins, while localizing electronic density in bonds rather than atomic sites. The other two outer layers in this model combine to describe the electrostatic Madelung potential of the zeolite framework. The middle layer is a set of partial atomic charges located at the zeolite atomic sites. This layer attempts to represent the local electrostatic interactions around the site of interest. These charge values can be obtained from periodic population analyses for similar systems, population analyses for the corresponding bare cluster, or the fraction or whole formal charges. The importance of the choice of these charges will be examined later in this work.

Due to the poor convergence properties of the Madelung potential, the explicit point charges in the middle layer, alone, are not able to accurately reproduce the crystal potential, so we add a set of surface charges, making up the outermost layer in our model. These surface charges are determined by the surface charge representation of the electrostatic embedding potential (SCREEP) method, which is described in more detail below. It allows replacement of the remainder of the Madelung potential with a small number of surface charges, with a resulting deviation of approximately 0.2 kJ/mol, from the true Madelung potential. Consequently, the main source of error in our model is located at the boundary between the quantum cluster and the explicit point charges.

The difficulty in this region is the strong interaction between the explicit point charges and the "artificial" saturating hydrogens of the cluster. This interaction is particularly strong with the first shell of explicit point charges (the set of point charges nearest to the quantum cluster—in our case the Si and Al charges next to the terminating hydrogens) since they are often less than one angstrom away from these hydrogens. Various schemes have been developed for minimizing these "boundary effects" in previous embedded cluster models: (1) adjust the value of this first shell of explicit point charges such that when combined with the charges of the artificial hydrogens, the Madelung potential at a point in the center of the cluster is reproduced;[17] (2) fit a series of charges around the quantum cluster so that, combined with the cluster, they reproduce the Madelung potential calculated at thousands of grid sites around the cluster, subsequently the boundary effect is minimized implicitly with this fit to the embedding potential;[19] (3) the Madelung potential is applied only to the central part of the quantum cluster;[18] and (4) adjust the position of this first shell of charges to minimize the boundary error.[26] In this study we accounted for these effects by simply removing this first shell of explicit point charges and distributing their charge among the second shell of explicit point charges (here, the second shell corresponds to the three O charges neighboring each Al and Si charge in the first shell). The effects of this approximation will be examined below.

Although the formulation of the SCREEP surface has been previously described in full detail,[27] for a complete description of our model we will give a brief overview of it here. First we draw a closed surface **S** such that all cluster atoms are in the interior of the surface. Then, based on a well-known theorem from electrostatics, no matter what the external charge distribution outside of **S** is, the electrostatic potential inside **S** can be rigorously replaced with some surface charge density ρ located on **S**. In practice the Ewald summation method is used to calculate the Madelung potential at points on **S** and then subtract the contribution from the explicit point charges to yield Φ_{diff} for these points. For computational reasons the boundary element method is employed to discretize **S** and represent ρ as a set of

TABLE 1: Environmental Embedding Charges (au)

atom type	STO-3G charges	6-21G charges	formal charges
H	0.21	0.49	1.00
Al	1.21	1.54	3.00
Si	1.42	2.03	4.00
O	−0.71	−1.015	−2.00

point charges **q** that satisfy the matrix equation **Aq = V**. Here the vector **V** contains values of Φ_{diff} at points $\mathbf{r}_j$ on the surface **S**, and **A** is the M × M nonsingular matrix with matrix elements

$$A_{ij} = \frac{1}{|\mathbf{r}_i - \mathbf{r}_j|} \text{ for } i \neq j \text{ and } A_{ii} = 1.07 \sqrt{4\pi/\mathbf{S}_i}$$

where $\mathbf{r}_i$ is the center of each surface element with area S_i.

Computational Details. Here we present the computational details that are common to all subsequent sections in this paper; details relating only to specific sections will be described therein. Chabazite's geometry was fixed to the structure resulting from an energy minimization within the shell model, using the parameters of Schröder,[28,29] with an Si/Al ratio of 3. We used the same $Si_2Al_2O_{13}H_{12}$ quantum cluster as Greatbanks et al.,[24] where dangling bonds were saturated by H with bond lengths of 1.00 Å and the OH groups were directed along the broken bonds. This cluster includes half of the 8-ring channel of chabazite. The values used for the embedding point charges are found in Table 1 and were derived from periodic calculations on chabazite using the STO-3G basis set,[30] a periodic calculation on sodalite using the 6-21G basis set, [31] and the formal values of the ions. Note that throughout the paper we define the adsorption energy as

$$E_{(adsorption)} = E_{(chabazite + NH_3)} - E_{(chabazite)} - E_{(NH_3)}$$

Binding energy is defined as the negative value of the adsorption energy, i.e., bound molecules will have positive binding energies and negative adsorption energies. The embedded cluster calculations were performed using our locally modified version of the G92/DFT program.[32] In this implementation of our embedding scheme we find only an additional 1−2% computational overhead compared to the corresponding bare cluster calculations.

Results

Accuracy of the Electrostatic Potential. First, we want to examine the accuracy of our model's representation of the Madelung potential in the QM region. In our chabazite model we used 199 surface charges and 1541 explicit point charges to achieve an RMS error of 0.3 kJ/mol in our representation of the Madelung potential; however, this is only a measure of the error arising from approximating the surface charge density (ρ) as a set of discrete point charges. The error due to our simple treatment of boundary effects, i.e., simply removing the point charges nearest to the capped hydrogens and dividing their charge among the next shell of point charges, is expected to be larger, so here we attempt to quantify this error. To get a better feel for the performance of our embedded cluster model, comparison with the cluster model is also provided.

We focused these analyses on three different contributions to the crystal potential. First, we examine the contribution due only to the boundary charges/atoms, between the quantum cluster and the surrounding crystal environment (just the terminating hydrogens in the cluster case). Second, since our treatment of boundary effects is static, it is important to examine variations in these effects due to changes in the electronic

structure of the system, i.e. how the electron density in the terminating hydrogens changes upon adsorption, and how these changes effect the potential inside the cluster region. Last, since the cluster method has no embedding environment, it is important to look at how well this method reproduces the Madelung potential in the cluster region.

To investigate the magnitude of deviations due to our treatment of boundary effects we used the potentials *at the Brønsted site* (since this is the most important region governing the adsorption process), due solely to the first shell of neighboring point charges, as reference values. We used charges derived from a Mulliken population analysis of a periodic HF/STO-3G calculation to generate these reference potentials. For our embedding scheme we arrived at these potential values by including contributions from the cap hydrogens (derived from Mulliken analyses of an embedded cluster calculation), as well as the charges added to the second shell of point charges, to see how well the sum of these contributions reproduced the potential due to the removed point charges. In the cluster case only the Mulliken charges of the cap hydrogens contribute to these potentials. In this comparison we find that our treatment of boundary effects results in an average deviation of 7.2% in the potential at the Brønsted site, while the cluster method's cap hydrogens yield an average deviation of 85% from that of the perfect crystal. Note that the cluster method's large deviation, here, does not indicate a poor representation of chabazite's potential in the cluster region, but instead just the inability of the terminating hydrogens to reproduce the electrostatics of the neighboring Al and Si sites which are not included in the cluster.

Because our treatment of these boundary effects is made a priori, it cannot respond to changes in the electron density of the terminal hydrogens in the formation of different adsorption complexes. To analyze the importance of this issue we repeated these analyses for the case of NH_4^+ adsorption in chabazite, as an example. In this case the Mulliken populations of the terminating hydrogens decreased by approximately 0.007 au, resulting in an average change of the potential at the Brønsted site by approximately 0.5% for our embedded cluster. This analysis indicates that this issue is negligible, especially considering that these results are for formation of an ion pair, which would create large changes in the electronic structure of the system.

To gain a better feel for the ability of the cluster method to reproduce chabazite's potential, we also compared the Madelung potential, or the finite electrostatic potential in the case of the bare cluster, at chabazite lattice sites within the quantum cluster region. We compared the potentials generated by a perfect chabazite crystal, our embedded cluster method, and the bare cluster results. In the perfect crystal case, the Madelung potential was calculated using the Ewald summation technique and the same Mulliken charges as those used above. For this series of calculations our embedding procedure, on average, reproduces a potential within 7.4% of the crystal Madelung potential, whereas the bare cluster results deviate by an average of 19%.

These results are particularly encouraging since here we were primarily concerned with verifying the practicality of the SCREEP representation for adsorbate studies in zeolites, and thus did not devote the effort to implementing a more rigorous treatment of boundary effects, yet we still were able to reproduce the Madelung potential reasonably well. Currently we are working on a rigorous treatment to reduce this error from boundary effects, which will be described in a forthcoming paper.

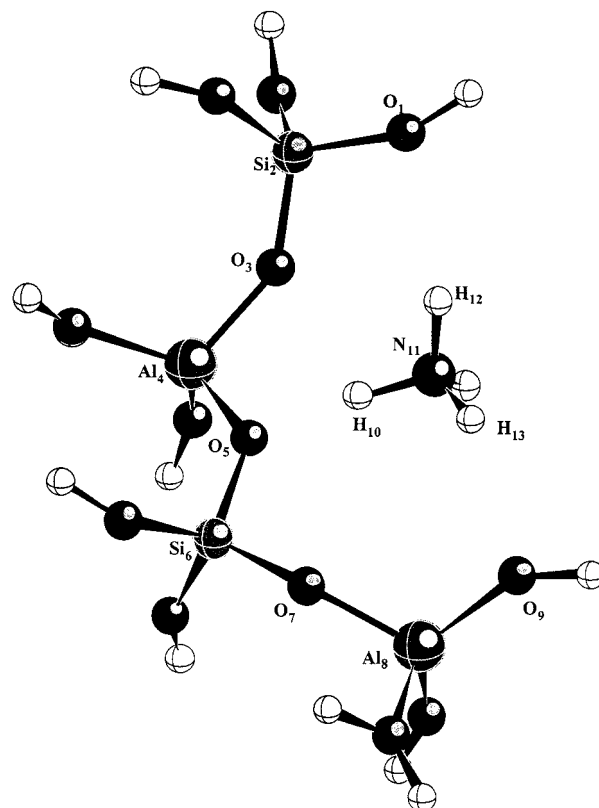**Comparison to Other Models.** To compare the accuracy of

Figure 2. Quantum mechanical 4T (four tetrahedral sites) cluster and NH_4^+ adsorbate.

our model with other embedded cluster models, periodic results, and bare cluster results, we performed the same potential energy scans as done in previous calculations on this system.[16,18,24] Specifically, we used the Hartree−Fock level of theory and STO-3G basis set to examine the head-on interaction of NH_3 and NH_4^+ with the neutral and anionic forms of the acidic chabazite, respectively. NH_3 and NH_4^+ were fixed at their experimental geometries,[33,34] and the structure of the anionic chabazite was not allowed to relax during the protonation process. The potential energy scans were generated by varying the $N_{11}-O_5$ distance with NH_3 and NH_4^+ principal axes directed along the O_5-H_{10} bond (see Figure 2).

Figure 3 displays the potential energy curves for NH_3 and NH_4^+ adsorption, calculated by different embedded cluster models (i.e., the present model and those from Pisani and Birkenheuer,[16] Teunissen et al.,[18] and Greatbanks et al.[24]) as well as the periodic HF[35] and bare cluster methods. All embedded cluster methods predict that NH_3 binds to the acidic site more tightly than the bare cluster results (ranging from 2 kJ/mol for Teunissen et al.'s method to 25 kJ/mol for EM-BED93). Our embedding scheme lies between these extremes and stabilizes the adsorption of NH_3 by about 18 kJ/mol over the bare cluster results and by approximately 12 kJ/mol over the periodic result. From this figure it is apparent that our method compares well with the other embedding procedures, as well as periodic HF, in its representation of the neutral pair complex in chabazite.

Regarding the adsorption of NH_4^+ on the anionic site of deprotonated chabazite, it has been stated previously that the STO-3G basis set is inadequate to properly model the ion pair structure (NH_4^+ adsorbed on deprotonated zeolite),[2] and, as will be demonstrated later, the optimized ion pair structure differs significantly from the head-on adsorption modeled here, so it is apparent that this is not an ideal model for the adsorption of
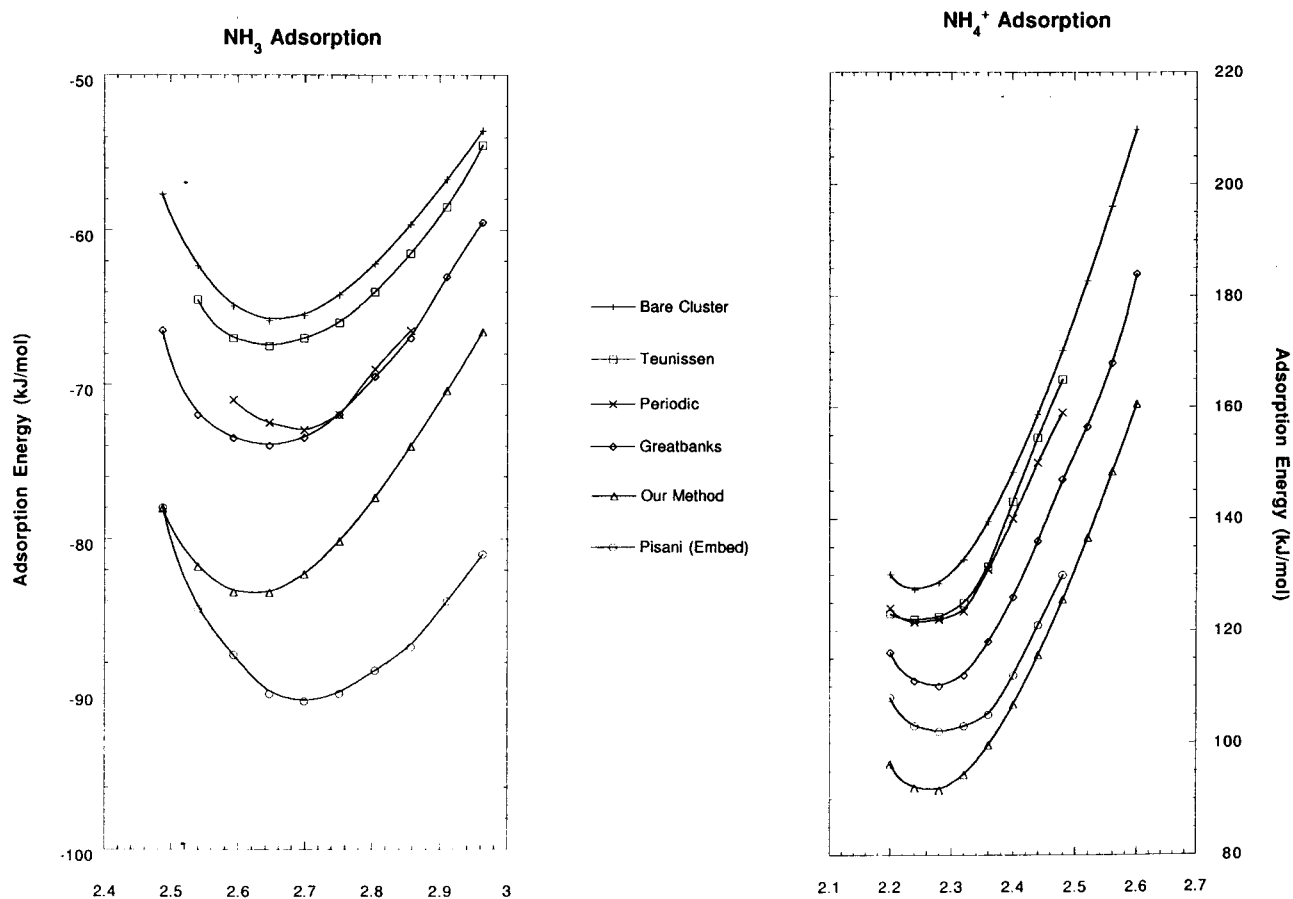
Figure 3. Calculated adsorption energy profiles, using various methods, for head-on adsorption of NH_3 and NH_4^+ in chabazite. The *x*-axis corresponds to the $N_{11}-O_5$ bond length in Å (see Figure 2 for labels).

NH_4^+. This model should, however, be satisfactory as a means of comparison to previous calculations on this system. Because of these deficiencies, these potential energy curves yield positive adsorption energy values (i.e., NH_4^+ is not bound) so here "NH_4^+ adsorption" refers only to the minima on these potential energy curves, and does not imply chemical binding. Again we find that the periodic results and all embedding schemes predict NH_4^+ to be "bound" more tightly than the bare cluster method's predicted adsorption energy of 127 kJ/mol. Teunissen et al.'s method and the periodic results both yield adsorption energies approximately 5 kJ/mol lower than that predicted by the bare cluster method, while Greatbanks et al. predict an NH_4^+ adsorption energy nearly 16 kJ/mol lower than the bare cluster result. Again our method compares most closely to Pisani and Birkenheuer's EMBED results, where both methods predict a strong stabilization of NH_4^+ adsorption, with respect to the bare cluster; EMBED predicts an adsorption energy about 24 kJ/mol lower than that of the bare cluster , while our method predicts an adsorption energy nearly 33 kJ/mol lower than the bare cluster results.

As can be seen from Figure 3, the previous embedded cluster studies deviate in their predicted adsorption energies by a relatively large amount (approximately 23 kJ/mol for the neutral pair and about 28 kJ/mol for the ion pair), leaving a bit of confusion as to which predicted value is the "best" for comparison. Typically, the periodic results are used as reference values in these comparisons; however, the periodic model does not represent a single adsorbate interacting with a chabazite Brønsted site, but an infinite array of adsorbates interacting with Brønsted acid sites, as well as with each other, corresponding to the high-loading case. Conversely, the embedded cluster

models represent a single adsorbate interacting with a chabazite Brønsted acid site, corresponding to the low-loading case; thus, we recommend using one of those models as a reference instead.

Of the previously proposed embedded cluster models, the models of both Teunissen et al. and Greatbanks et al. include only the electrostatic contributions of the crystal environment, whereas, Pisani and Birkenheuer's EMBED results include the electrostatics, as well as quantum contributions from the crystal environment, so we propose that they may provide the best reference values for this comparison. In both the NH_3 and NH_4^+ adsorption processes, the periodic method yields lower binding energies than the EMBED method, which agrees with experiment, where it is nearly always seen that an isolated adsorption site binds an adsorbate more tightly than in the high-loading case. Our predictions also indicate tighter bindings than those predicted with the periodic method, and compare well with Pisani and Birkenheuer's EMBED predictions (within 7 kJ/mol for NH_3 and 9 kJ/mol for NH_4^+). The other embedded cluster methods, however, do not agree as well. In both the neutral pair and ion pair cases, their predicted adsorption energies deviate by as much as 23 kJ/mol from the EMBED predictions. We believe these deviations could be due to two factors.

First, these comparisons are not made at true stationary states on the potential energy surface, so what might normally be slight topological variations between the methods ends up yielding large differences in relative energies since they are not being compared at good reference points. Second, these deviations may also hint at errors in the method's representation of the electrostatic potential. For example, above we found that, on average, our embedded cluster model deviates from chabazite's Madelung potential by 7.4%, whereas, the bare cluster model

TABLE 2: Effect of Environmental Embedding Charges on Adsorption Energies, E_{ads} (kJ/mol), and Equilibrium N−O Distances, N−O$_{eq}$ (Å), for Head-On Adsorption

	charges			
	cluster	STO-3G	6-21G	formal
NH$_3$ adsorption				
E_{ads}	−65.9	−83.6	−91.8	−109.7
N−O$_{eq}$	2.65	2.60	2.60	2.60
NH$_4^+$ adsorption				
E_{ads}	127.4	91.6	75.5	39.1
N−O$_{eq}$	2.24	2.28	2.28	2.28

deviates by 19%. NH$_4^+$/chabazite adsorption is primarily governed by electrostatics, so we would expect these deviations in representations of the Madelung potential to carry over to predicted binding energies for this reaction. Then, using Pisani and Birkenheuer's EMBED results as a reference, a 7.4% deviation from their predicted adsorption energy of 102 kJ/mol would correspond to a deviation of approximately 8 kJ/mol. We find a difference of 9 kJ/mol between our predicted adsorption energy and the EMBED result. A 19% deviation from 102 kJ/mol would correspond to approximately 19 kJ/mol, which is also reasonably close to the 25 kJ/mol difference between the bare cluster and EMBED predictions.

Effects of the Environmental Ionicity. As mentioned previously, the effect of the environmental embedding charges on adsorption energies needs to be more thoroughly examined. For simple zeolite structures such as chabazite or sodalite these charges can be derived from previous periodic calculations; however, different basis sets can deviate significantly in their predicted ionicities for the system. In more complicated systems the situation is more difficult because periodic calculations are not feasible, so these charges must be estimated in some manner. In this case, understanding the magnitude of this effect can yield valuable insight into the quality of estimates required to achieve reliable results.

We investigate the importance of this choice by optimizing the N$_{11}$−O$_5$ distance for NH$_3$ and NH$_4^+$ head-on adsorption, using three different sets of environmental charges (found in Table 1), as well as no embedding. Table 2 presents the results for varying the ionicity of the environment on the head-on adsorption of NH$_3$ at a Brønsted site in chabazite. This table shows a slight shortening of N−O$_{eq}$ (0.05 Å), for the adsorption complex, with increasing environmental ionicities. There is a much stronger effect on adsorption energies. Each set of charges predicts NH$_3$ to bind more tightly to chabazite than do the bare cluster predictions, with an increase in binding energy from 17.7 kJ/mol with the STO-3G environmental charges to 25.9 kJ/mol for the 6-21G charges to 43.8 kJ/mol with the formal charges. On the basis of these results we see that an increase in the environmental ionicity by 1 au stabilizes NH$_3$ adsorption by approximately 22 kJ/mol; therefore, as long as we estimate the environmental charges for a neutral pair system within 1 au of the "true" value, we can place approximate error limits of 22 kJ/mol on the results for that system (of course neglecting the errors due to the standard approximations in computational methods). In practice we expect to achieve much better estimates for the environmental charges than 1 au since it has been noted previously that the charges calculated for periodic structures and cluster models are "virtually identical" (most reported deviations were much smaller than 0.02 au).[2]

As in the neutral pair complex, we do not see much effect of the environmental charges on the equilibrium geometry for the head-on attack of NH$_4^+$, except for a slight increase in N−O$_{eq}$ (0.04 Å). In energetic terms the environmental charges have a

TABLE 3: Optimized Geometries for the Bare Cluster and Various Embedding Schemes (Distances are in Å and Angles in Degrees)

	cluster	SCREEP STO-3G	SCREEP 6-21G	SCREEP formal	Teunissen[4]
chabazite					
framework					
O$_3$−Al$_4$	1.74	1.69	1.68	1.67	
Al$_4$−O$_5$	1.89	1.89	1.89	1.88	1.87
O$_5$−Si$_6$	1.73	1.72	1.72	1.74	1.68
Si$_6$−O$_7$	1.61	1.59	1.58	1.56	
O$_5$−H$_{10}$	0.98	0.96	0.97	0.97	0.96
∠Al$_4$O$_5$Si$_6$	120.9	132.4	132.8	133.8	136/139
chabazite + NH$_4^+$					
O$_3$−A$_{14}$	1.75	1.72	1.71	1.70	
Al$_4$−O$_5$	1.79	1.78	1.77	1.76	1.77
O$_5$−S$_{i6}$	1.65	1.63	1.63	1.64	1.61
Si$_6$−O$_7$	1.63	1.61	1.61	1.59	
O$_5$−H$_{10}$	1.73	1.58	1.62	1.72	1.50
H$_{12}$−O$_1$	1.80	2.48	2.52	2.74	
H$_{13}$−O$_9$	1.79	2.38	2.33	2.17	
∠Al$_4$O$_5$Si$_6$	133.1	133.1	134.0	136.0	140/141

more significant effect on the ion pair structures than the neutral pair complexes. Specifically, the predicted NH$_4^+$ binding energies are higher than the bare cluster predictions, ranging from an increase of 35.8 kJ/mol with the STO-3G environmental charges to 51.9 kJ/mol for the 6-21G charges to 88.3 kJ/mol with the formal charges. If we estimate the dependence of adsorption energies on the environmental charges, for the ion pair complex, we get an error estimate of approximately 44 kJ/mol for 1 au deviation in the environmental charges. Note that this effect for the ion pair complex is approximately twice that for the neutral pair complex.

Geometry Optimizations. In this subsection we attempt to achieve more quantitative results for the chabazite/NH$_3$ system by (1) allowing part of the QM cluster to relax during the adsorption process, (2) using a larger basis set, (3) including electron correlation, and (4) accounting for the basis set superposition error and zero-point energy in our final adsorption energies. In our geometry optimization, the terminal OH groups were held fixed, but the remaining framework atoms of the QM cluster and the adsorbate were completely relaxed. The HF/CEP-31G level of theory was used for the geometry optimizations. The same three sets of embedding charges as above were used for the optimizations. To obtain an estimate for the effects of electron correlation we performed a single point calculation at the optimized structure using the B3LYP/CEP-31G method.

We were able to find an optimized structure for the NH$_4^+$/chabazite complex, where the NH$_4^+$ was tightly complexed to the chabazite wall with three hydrogen bonds. This structure is consistent with experimental observation.[36] Table 3 shows the optimized parameters for the chabazite cluster with and without adsorbate and demonstrates the changes in the zeolite's structure during the adsorption process, as well as the dependence on the ionicity of the environment. To see the absolute effect of the embedding we have attempted to repeat these optimizations for the bare cluster; however, without the stabilization of the embedding environment the presence of adsorbate "tears" the cluster away from the fixed terminal OH groups, leaving isolated OHs. So instead we performed *full* geometry optimizations for the bare cluster (without the constraints on the terminating OH groups or adsorbate) to get some estimate for treating chabazite as an isolated H$_{12}$Al$_2$Si$_2$O$_{13}$ cluster.

These results demonstrate that the Madelung field has little effect on the structure of the cluster framework atoms, since the geometries are so similar for these atoms for all sets of

TABLE 4: Adsorption Energies (kJ/mol) for NH_4^+ Adsorption in Chabazite, Calculated Using Various Embedding Schemes

method	bare cluster	relaxed cluster	SCREEP (STO-3G)	SCREEP (6-21G)	SCREEP (formal)	Teunissen's[4] cluster	Teunissen[4]
HF	−113	−137	−151	−168	−207	−31	−48
HF/CPC	−108	−132	−147	−166	−204	−5	−28
B3LYP	−144	−170	−174	−190	−225	−67	−84
B3LYP/CPC	−139	−165	−172	−190	−225	−36	−50
B3LYP/CPC/ZPE	−119	−145	−152	−170	−205		

environmental charges. The positioning of the adsorbate, however, is affected significantly by the Madelung potential. In the relaxed bare cluster optimizations the NH_4^+ cation is stabilized via three relatively strong H-bonds (rOH ranging from 1.73 to 1.80 Å) with the zeolite framework. In contrast, the embedded cluster results predict the formation of one strong ($rO_5H_{11} = 1.62$ Å with the 6-21G charges) and two weak (2.33, 2.52 Å) H-bonds to stabilize the NH_4^+. The symmetric H-bonds of the bare cluster geometry unrealistically "pinch" chabazite's cavity about the adsorbate, effectively shrinking the channel's diameter by 1.77 Å. We also found that the environmental charges have large effects on the placement of the ammonium ion in the zeolite cavity. Specifically, with increasing ionicity the ammonium ion moves further from Al_4 and closer to Al_8 ($rN_{11}Al_8$ decreases from 3.83 to 3.72 Å when the formal charges are used instead of the STO-3G charges).

Adsorption energies for NH_4^+ in chabazite, calculated at different levels of theory and using different embedded cluster models, are listed in Table 4. Again all embedded results predict higher binding energies for NH_4^+ adsorption than the cluster method's prediction of 119 kJ/mol. The STO-3G charges yield binding energies 33 kJ/mol higher than the bare cluster method, whereas the 6-21G charges give results higher by 51 kJ/mol and the formal charges by 86 kJ/mol. Again, if we try to extrapolate a dependence of binding energies on the environmental charges we arrive at a value of approximately 47 kJ/mol au, which is in good agreement with our previous estimate for the ion pair complex.

Allowing the bare cluster to completely relax stabilizes the adsorbate by an additional 26 kJ/mol, yielding a more reasonable binding energy of 145 kJ/mol. This value is close to that predicted by our embedding scheme with the STO-3G environmental charges (152 kJ/mol) but underestimates our 6-21G results by 25 kJ/mol; however, this additional stabilization is achieved at the cost of distorting the cluster from the chabazite structure to an unrealistic degree.

Discussion

We were unable to find any reported experimental values for the heat of adsorption of NH_3 on H-chabazite; however, it is possible to apply the Redhead method[37] to TPD data for this system[25] to estimate the heat of adsorption. One parameter which is not available for this analysis is the preexponential factor (ν) for this system, in which case one normally uses the value of 1×10^{13} s^{-1} for ν (assuming a tight transition state for the desorption process). Instead of using this default value, however, we thought a better estimate would be to use preexponential factors reported for NH_3 desorption in H-ZSM-5 (ranging from 4.89×10^{11} to 1.35×10^{12}s^{-1}).[38] With this assumption, the Redhead analysis yields −154 to −164 kJ/mol as a rough estimate for the heat of adsorption for NH_3 on H-chabazite. This estimate seems reasonable since it is known that most zeolite Brønsted sites protonate NH_3 to NH_4^+, with a heat of adsorption in the range of −150 ± 35 kJ/mol.[4] Due to the small channel size of chabazite (3.8 Å), and since the NH_4^+ is known to be

highly complexed to the zeolite wall, we expect a heat of adsorption a little toward the upper limit of this range.

Teunissen et al. is the only other group to attempt geometry optimizations on the chabazite/NH_3 system, and Table 3 compares our geometries with their results.[4] Note that because of the constraints that Teunissen et al. placed on their geometry for NH_4^+ adsorption, we cannot compare directly for the position of the adsorbate; however, their framework geometry compares well with our results. Table 4 compares the energetics of our optimized structures, at various levels of theory, with that of Teunissen et al. Here we present the results of our embedding scheme using all three sets of environmental charges; however, we believe that the 6-21G charges give the best description of the zeolite ionicity and we expect them to give the most reliable results. For the zero-point energy (ZPE) estimate we use the zero-point energy calculated for the fully relaxed $H_{12}Al_2Si_2O_{13}$ cluster (20.1 kJ/mol). It is interesting to note that after including electron correlation, the counterpoise correction (CPC), and zero-point energy, we arrive at adsorption energies within 2 kJ/mol of the original Hartree−Fock predictions. These predictions range from −152 kJ/mol using the STO-3G charges to −205 kJ/mol for the formal charges. The 6-21G charges yield a final heat of adsorption of −170 kJ/mol, in good agreement with our estimates of −154 to −164 kJ/mol based on Beyer et al.'s TPD data.

Teunissen et al.'s predictions, without their error estimates, drastically underestimate the adsorption of NH_4^+ to chabazite. Their optimized structure, including estimates for electron correlation (with the MP2 method) and the counterpoise correction, yields an adsorption energy of −50 kJ/mol. They made error estimates (due to basis set deficiencies, incomplete van der Waals energy, partial optimization, and errors made with the optimization at the RHF level) to be 70 ± 15 kJ/mol, where 40−50 kJ/mol of this error is due to the limited basis set size. Examining Table 4, where we look at the adsorption energies for our cluster, without embedding, and the cluster used by Teunissen et al., we propose that a majority of Teunissen et al.'s error is instead due to constraints on their geometry optimization and choice of cluster, since we find that our bare cluster binds NH_3 more tightly than theirs by 103 kJ/mol, after considering the CPC.

Conclusions

We have presented an embedded cluster methodology for studying interactions in zeolites and have examined NH_3 adsorption at Brønsted acid sites in chabazite, in an effort to validate this model. We have found that the Madelung potential is important for obtaining quantitative results for adsorption structures and energies. The Madelung potential depends strongly on the environmental charges used; however, we found that with minimal error these charges can be estimated from cluster calculations rather than expensive periodic calculations. For the NH_3/chabazite system, structure relaxation was found to be necessary to predict NH_4^+ adsorption to be favorable. With inclusion of structure relaxation, electron correlation, basis set

superposition errors, and zero-point energy corrections, we calculated a final heat of adsorption of -170 kJ/mol, in good agreement with TPD data (-154 to -164 kJ/mol). [25]

Overall, this embedded cluster model seems very promising for the study of zeolite/adsorbate interactions. Because this embedding scheme adds minimal computational overhead (1$-$2%) over that required for the QM cluster, reasonably large regions of the zeolite can be modeled quantum mechanically, as well as intermediate adsorbates; thus, it is possible to model reactions in zeolites with a high level of accuracy.

References and Notes

(1) Sauer, J. *Chem. Rev.* **1989**, *89*, 199.

(2) Sauer, J.; Ugliengo, P.; Garrone, E.; Saunders: V. R. *Chem. Rev.* **1994**, *94*, 2095.

(3) van Santen, R. A.; Kramer, G. J. *Chem. Rev.* **1995**, *95*, 637.

(4) Teunissen, E. H.; Jansen, A. P. J.; van Santen, R. A. *J. Phys. Chem.* **1995**, *99*, 1873.

(5) van Santen, R. A.; de Man, A. J. M.; Jacobs, W. P. J. H.; Teunissen, E. H.; Kramer, G. J. *J. Catal. Lett.* **1991**, *9*, 273.

(6) Stock, T.; Dombrowski, D.; Fruwert, J. *Z. Phys. Chem. (Leipzig)* **1984**, *3-6*, 738.

(7) Jacobs, W. P. J. H.; van Wolput, J. H. M. C.; van Santen, R. A. *J. Chem. Soc., Faraday Trans.* **1993**, *89*, 1271.

(8) Jacobs, W. P. J. H.; van Wolput, J. H. M. C.; van Santen, R. A. *Zeolites* **1993**, *13*, 170.

(9) Earl, W. L.; Fritz, P. D.; Gibson, A. A. V.; Lunsford, J. H. *J. Phys. Chem.* **1987**, *91*, 2091.

(10) Michel, D.; Germanus, A.; Pfeifer, H. *J. Chem. Soc., Faraday Trans.* **1982**, *78*, 237.

(11) Vega, A. J.; Luz, Z. *J. Phys. Chem.* **1987**, *91*, 365.

(12) Deininger, D.; Reïman, B. *Z. Phys. Chem. (Leipzig)* **1972**, *251*, 351.

(13) Gibbs, G. V.; Meagher, E. P.; Newton, M. D.; Swanson, D. K. *Structure and Bonding in Crystals*; Academic: New York, 1981; Vol. 1, p 195.

(14) Gibbs, G. V. *Am. Mineral.* **1982**, *67*, 421.

(15) Mezey, P. G., Eds. *Catalytic Materials: Relationship Between Structure and Reactivity*; American Chemical Society: Washington, D.C., 1984; p 145.

(16) Pisani, C.; Birkenheuer, U. *Int. J. Quantum Chem.* **1995**, *S29*, 221.

(17) Allavena, M.; Seiti, K.; Kassab, E.; Ferenczy, G.; Angyan, J. G. *Chem. Phys. Lett.* **1990**, *168*, 461.

(18) Teunissen, E. H.; Jansen, A. P.; van Santen, R. A.; Orlando, R.; Dovesi, R. *J. Chem. Phys.* **1994**, *101*, 5865.

(19) Greatbanks, S. P.; Sherwood, P.; Hillier, I. H. *J. Phys. Chem.* **1994**, *98*, 8134.

(20) Maseras, F.; Morokuma, K. *J. Comput. Chem.* **1995**, *16*, 1170.

(21) Brändle, M.; Sauer, J. *J. Mol. Catal. A: Chem.* **1997**, *119*, 19.

(22) Shapovalov, V.; Stefanovich, E. V.; Truong, T. N. *J. Phys. Chem.* **1998**, submitted.

(23) Stefanovich, E. V.; Truong, T. N. *Chem. Phys. Lett.* **1999**, *299*, 623.

(24) Greatbanks, S. P.; Hillier, I. H.; Sherwood, P. *J. Comput. Chem.* **1997**, *18*, 562.

(25) Beyer, H. K.; Jacobs, P. A.; Uytterhoeven, J. B. *J. Chem. Soc., Faraday Trans. 1* **1976**, *73*, 1111.

(26) Vetrival, R.; Catlow, C. R. A.; Colbourn, E. A. In *Studies in Surface Science and Catalysis*; Grobet, P. J.; Mortier, W. J.; Vansant, E. F.; Schalz-Ekloff, G., Eds.; Elsevier: Amsterdam, 1988; Vol. 37; p 309.

(27) Stefanovich, E. V.; Truong, T. N. *J. Phys. Chem. B* **1998**, *102*, 3018.

(28) Schröder, K.; Sauer, J.; Leslie, M.; Catlow, C. R. A.; Thomas, J. M. *Chem. Phys. Lett.* **1992**, *188*, 320.

(29) Schröder, K.; Sauer, J.; Leslie, M.; Catlow, C. R. A. *Zeolites* **1992**, *12*, 20.

(30) Greatbanks, S. P., personal communication.

(31) Nicholas, J. B.; Hess, A. C. *J. Am. Chem. Soc.* **1994**, *116*, 5428.

(32) Frisch, M. J.; Trucks, G. W.; Schlegel, H. B.; Gill, P. M. W.; Johnson, B. G.; Wong, M. W.; Foresman, J. B.; Robb, M. A.; Head-Gordon, M.; Replogle, E. S.; Gomperts, R.; Andres, J. L.; Raghavachari, K.; Binkley, J. S.; Gonzalez, C.; Martin, R. L.; Fox, D. J.; Defrees, D. J.; Baker, J.; Stewart, J. J. P.; Pople, J. A. *GAUSSIAN 92/DFT*, Gaussian, Inc.: Pittsburgh, PA, 1993.

(33) Herzberg, G. *Molecular Spectra and Molecular Structure*; Van Nostrand: Princeton, NJ, 1945; Vol. 2.

(34) Ibers, J. A.; Stevenson, D. P. *J. Chem. Phys.* **1958**, *28*, 929.

(35) Teunissen, E. H.; Roetti, C.; Pisani, C.; deMan, A. J. M.; Jansen, A. P. J.; Orlando, R.; van Santen, R. A.; Dovesi, R. *Model. Sim. Mater. Sci. Eng.* **1994**, *2*, 921.

(36) Stuckenschmidt, E.; Kassner, D.; Joswig, W.; Baur, W. H. *J. Mineral.* **1992**, *4*, 1229.

(37) Redhead, P. A. *Vacuum* **1962**, *12*, 203.

(38) Hunger, B.; Hoffmann, J.; Heitzsch, O.; Hunger, M. *J. Therm. Anal.* **1990**, *36*, 1379.